Potential of Brillouin scattering in polymer optical fiber for strain-insensitive high-accuracy temperature sensing

Yosuke Mizuno* and Kentaro Nakamura

Precision and Intelligence Laboratory, Tokyo Institute of Technology, 4259 Nagatsuta, Midori-ku, Yokohama 226-8503, Japan

**Corresponding author: ymizuno@sonic.pi.titech.ac.jp*

Received September 20, 2010; accepted October 23, 2010;
posted November 1, 2010 (Doc. ID 135374); published November 23, 2010

We investigated the dependences of Brillouin frequency shift (BFS) on strain and temperature in a perfluorinated graded-index polymer optical fiber (PFGI-POF) at 1.55 μm wavelength. They showed negative dependences with coefficients of −121.8 MHz/% and −4.09 MHz/K, respectively, which are −0.2 and −3.5 times as large as those in silica fibers. These unique BFS dependences indicate that the Brillouin scattering in PFGI-POFs has a big potential for strain-insensitive high-accuracy temperature sensing. © 2010 Optical Society of America

OCIS codes: 060.2370, 130.5460, 290.5830.

Brillouin scattering [1,2] is a fundamental nonlinear optical process in fiber-optic communication systems and has been widely studied. So far, many useful applications have been reported, such as microwave signal processing, slow-light generation, phase conjugation, tunable delay, and strain/temperature sensing [3–5]. On the other hand, polymer optical fibers (POFs) [6–8] are highly flexible and offer extremely easy and low-cost connection compared to other standard glass fibers. In spite of their higher loss than that of silica fibers, POFs have been used in medium-range communication applications, such as home networks and automobiles, as well as in high-strain monitoring applications [8]. Recently, we have reported on the observation of Brillouin scattering in a perfluorinated graded-index polymer optical fiber (PFGI-POF) at 1.55 μm [9]. The Brillouin frequency shift (BFS) was about 2.83 GHz, and the calculated Brillouin gain coefficient g_B of 3.09×10^{-11} m/W was comparable to that of silica fibers. This indicated that, as Brillouin scattering in silica fibers has a wide field of application, Brillouin scattering in POFs can also be exploited for a variety of practical devices and systems with their low cost, ease of installation, and high flexibility.

In this Letter, for sensing applications, we investigate the dependences of the BFS on strain and temperature in the PFGI-POF at 1.55 μm. It is found that the BFS in the PFGI-POF moves toward lower frequency with increasing strain and temperature and that their coefficients are −121.8 MHz/% and −4.09 MHz/K, respectively. Compared to the coefficients of +580 MHz/% and +1.18 MHz/K in silica fibers, their absolute values are 0.2 and 3.5 times as large, respectively. These unique BFS dependences seem to be caused by the unique dependences of the Young's modulus on strain and temperature in the PFGI-POF. We believe Brillouin scattering in PFGI-POFs can be potentially utilized to develop strain-insensitive high-accuracy temperature sensors.

When a light beam is injected into an optical fiber, backscattered light (Stokes light) is generated through the interaction with acoustic phonons. This phenomenon is called the spontaneous Brillouin scattering. Since the phonons decay exponentially, the backscattered Brillouin light spectrum, also known as the Brillouin gain spectrum (BGS), takes the shape of a Lorentzian function. The frequency at which the peak power is obtained in the spectrum is downshifted for several gigahertz from the incident light frequency, and the amount of this frequency shift is known as BFS. In optical fibers, the BFS ν_B is given as [2]

$$\nu_B = \frac{2n\nu_A}{\lambda_p} = \frac{2n}{\lambda_p}\sqrt{\frac{E}{\rho}}, \tag{1}$$

where n is the refractive index, ν_A is the acoustic velocity in the fiber, λ_p is the wavelength of the incident pump light, E is the Young's modulus, and ρ is the density. If tensile strain or temperature changes in a standard silica single-mode optical fiber (SMF), the BFS moves to higher frequency in proportion to the applied strain (+580 MHz/%) [10] and the temperature change (+1.18 MHz/K) [11]. In some specialty fibers, such as tellurite glass fibers, it is known that the BFS moves to lower frequency with increasing applied strain (−230 MHz/%) [12] and temperature (−1.14 MHz/K) [13]. In either case, by measuring the BFS in the fiber, the strain amplitude or temperature change can be derived.

We employed a 5 m PFGI-POF [9,14] with an NA of 0.185, a core diameter of 120 μm, a core refractive index of ∼1.35, and a propagation loss of ∼150 dB/km at 1.55 μm. The experimental setup for investigating the BFS dependence on strain and temperature in the PFGI-POF is basically the same as that previously reported in [9], where heterodyne detection was used to observe the BGS with a high resolution, and one end of the PFGI-POF was connected to the silica SMF by so-called butt coupling. The other end was kept open. Though the Stokes light includes the Brillouin signal caused in the 1 m SMF between the circulator and the PFGI-POF, it has no influence on the BGS measurement, because the BFS in the SMF is about four times higher than that in the PFGI-POF [9]. Different strains were applied to the whole length of the PFGI-POF fixed on a translation stage using epoxy glue, while the temperature along the whole length of the PFGI-POF was adjusted with a heater.

 © 2010 Optical Society of America

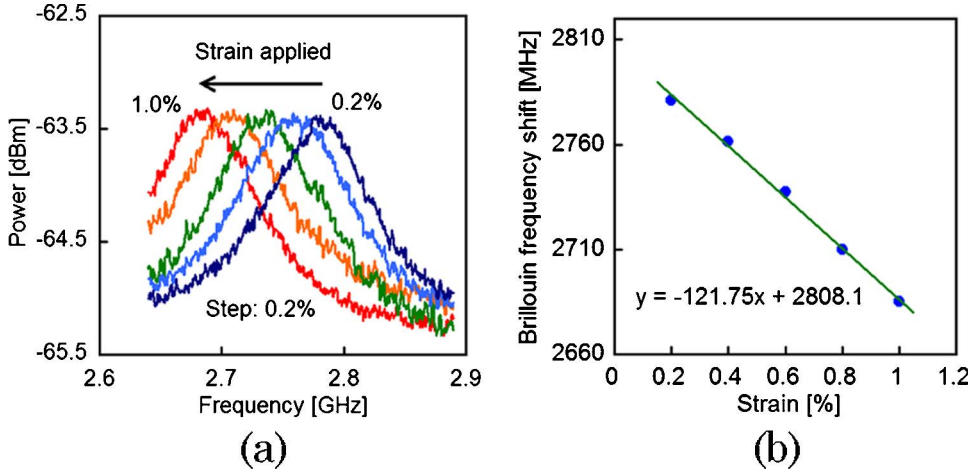

Fig. 1. (Color online) Measured dependences of (a) the BGS and (b) the BFS on strain in the PFGI-POF.

The strain dependence of the BGS in the PFGI-POF is shown in Fig. 1(a). The pump power was 19 dBm, and strains of 0.2, 0.4, 0.6, 0.8, and 1.0% were applied. With the increasing applied strain, the BGS shifted toward lower frequency. Figure 1(b) shows the strain dependence of the BFS. The slope was almost linear, and its coefficient was calculated to be −121.8 MHz/%. While the negative sign is the same as in tellurite glass fibers [12], the absolute value was about one fifth of that of a standard silica SMF (+580 MHz/%) [10].

Then, the temperature dependence of the BGS in the PFGI-POF is shown in Fig. 2(a). The pump power was 23 dBm, and the temperature was controlled from 30 °C up to 80 °C with a step of 10 °C. With increasing temperature, the BGS also shifted toward lower frequency. The Stokes power at high temperature over 40 °C was lower than that at 30 °C by about 0.7 dB, probably due to the nonuniform temperature distribution on the heater. Figure 2(b) shows the temperature dependence of the BFS, from which its coefficient was calculated to be −4.09 MHz/K. Though the negative sign is also the same as in tellurite glass fibers [13], the absolute value was about 3.5 times as large as that of an SMF (+1.18 MHz/K) [11].

The smaller strain coefficient indicates that PFGI-POF-based Brillouin sensors are less susceptible to the applied strain. On the other hand, the larger temperature coefficient leads to accuracy enhancement of the temperature measurement. Thus, the Brillouin scattering in the PFGI-POF can be potentially utilized in strain-insensitive high-accuracy temperature sensors.

Next, the origins of the unique BFS dependences on strain and temperature in the PFGI-POF are discussed. The strain coefficient of the normalized BFS is expressed, by differentiating Eq. (1) with respect to strain, as

$$\frac{1}{\nu_B}\frac{\partial \nu_B}{\partial \varepsilon} = \frac{1}{n}\frac{\partial n}{\partial \varepsilon} + \frac{1}{2E}\frac{\partial E}{\partial \varepsilon} + \left(-\frac{1}{2\rho}\frac{\partial \rho}{\partial \varepsilon}\right). \tag{2}$$

Here it is known that the following equations hold true [10]:

$$\frac{1}{n}\frac{\partial n}{\partial \varepsilon} = -n^2\frac{p_{12} - \kappa(p_{11} + p_{12})}{2}, \tag{3}$$

$$-\frac{1}{\rho}\frac{\partial \rho}{\partial \varepsilon} = \frac{1 - 2\kappa}{2}, \tag{4}$$

where p_{11} and p_{12} are the elasto-optic coefficients and κ is the Poisson's ratio. Since their values in PFGI-POF

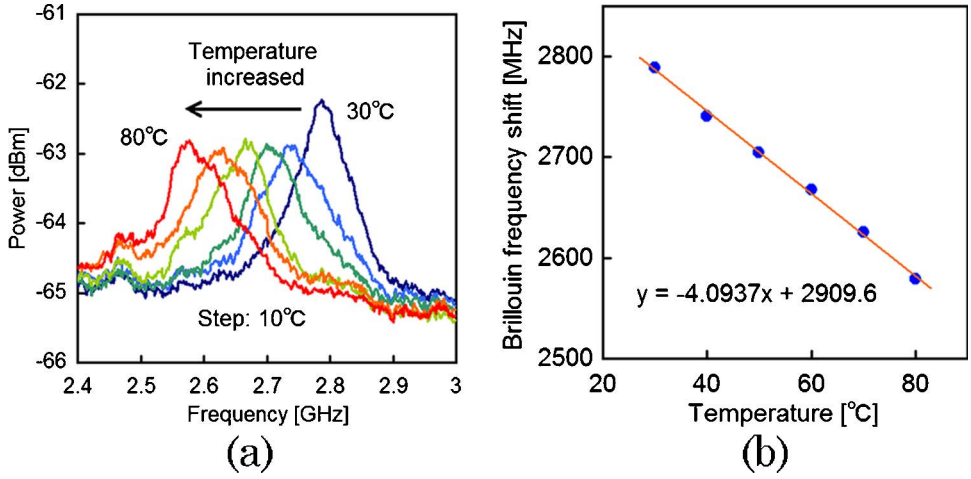

Fig. 2. (Color online) Measured dependences of (a) the BGS and (b) the BFS on temperature in the PFGI-POF.

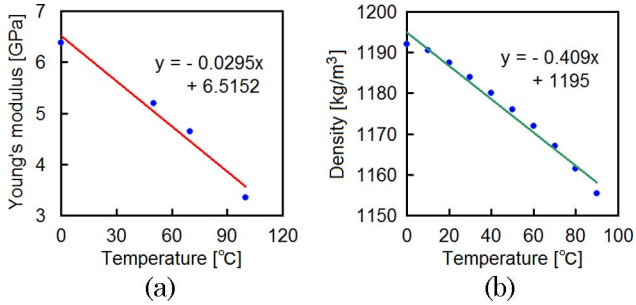

Fig. 3. (Color online) Temperature dependences of (a) the Young's modulus and (b) the density of bulk PMMA, plotted using the data reported in [19].

are unknown, we used the values for bulk polymethyl methacrylate (PMMA): $p_{11} = 0.3$ [15], $p_{12} = 0.297$ [15], and $\kappa = 0.34$ [16]. Then, the first and the third terms in Eq. (2) were calculated to be −0.0857 and +0.16, respectively. Though the second term is reported to vary drastically depending on the method to apply strain as well as on the fabrication quality of the fiber, we used −5.75 as the second term, which is the value reported in [17] for a standard PMMA-based POF. Its absolute value is much larger than the first and the third terms. Then, the theoretical strain coefficient was calculated to be −160.6 MHz/%. Considering that each term in Eq. (2) was estimated using the values of PMMA, this value is in moderate agreement with the experimental value of −121.8 MHz/%. Thus, the unique strain dependence of the BFS seems to originate from the unique dependence of the Young's modulus on strain in the PFGI-POF.

Finally, we discuss the BFS dependence on temperature in the same way. The temperature coefficient of the normalized BFS is given as

$$\frac{1}{\nu_B}\frac{\partial \nu_B}{\partial T} = \frac{1}{n}\frac{\partial n}{\partial T} + \frac{1}{2E}\frac{\partial E}{\partial T} + \left(-\frac{1}{2\rho}\frac{\partial \rho}{\partial T}\right). \tag{5}$$

The first term can be calculated to be −0.0000889 using the value reported for a standard PMMA-based POF [18]. To estimate the second and the third terms, we plotted the Young's modulus and the density of bulk PMMA at various temperatures that have been reported in [19], as shown in Figs. 3(a) and 3(b). Using their slopes (−0.0295 GPa/K and −0.409 kg/m^3/K), along with $E \sim 6$ GPa and $\rho = 1187.5$ kg/m^3, the second and the third terms were calculated to be −0.00246 and +0.000172, respectively. Then, the theoretical temperature coefficient was calculated to be −6.72 MHz/K, which roughly agrees with the experimental value of −4.09 MHz/K. Thus, the unique temperature dependence of the BFS also seems to be caused by the large negative dependence of the Young's modulus on temperature in the PFGI-POF.

In conclusion, the BFS dependences on strain and temperature in a 5 m PFGI-POF were investigated at 1.55 μm wavelength. They showed negative dependences with coefficients of −121.8 MHz/% and −4.09 MHz/K, respectively, which are −0.2 and −3.5 times as large as those in silica fibers. With these unique BFS dependences, probably caused by the unique dependences of the Young's modulus on strain and temperature, we believe the Brillouin scattering in PFGI-POFs has a big potential for strain-insensitive high-accuracy temperature sensing systems. The next step needed to implement such systems is to enhance the Stokes power, for example, by reducing the core diameter of the PFGI-POFs.

We are indebted to Prof. Nishiyama and Prof. Uenohara of Tokyo Institute of Technology, Japan, for lending us their high-power erbium-doped fiber amplifiers. Y. Mizuno is grateful to the Research Fellowships for Young Scientists from the Japan Society for the Promotion of Science (JSPS).

References

1. E. P. Ippen and R. H. Stolen, Appl. Phys. Lett. **21**, 539 (1972).
2. G. P. Agrawal, *Nonlinear Fiber Optics* (Academic Press, 1995).
3. T. Horiguchi and M. Tateda, J. Lightwave Technol. **7**, 1170 (1989).
4. K. Hotate and T. Hasegawa, IEICE Trans. Electron. **E83-C**, 405 (2000).
5. Y. Mizuno, W. Zou, Z. He, and K. Hotate, Opt. Express **16**, 12148 (2008).
6. M. G. Kuzyk, *Polymer Fiber Optics: Materials, Physics, and Applications* (CRC Press, 2006).
7. Y. Koike, T. Ishigure, and E. Nihei, J. Lightwave Technol. **13**, 1475 (1995).
8. I. R. Husdi, K. Nakamura, and S. Ueha, Meas. Sci. Technol. **15**, 1553 (2004).
9. Y. Mizuno and K. Nakamura, Appl. Phys. Lett. **97**, 021103 (2010).
10. T. Horiguchi, T. Kurashima, and M. Tateda, IEEE Photonics Technol. Lett. **1**, 107 (1989).
11. T. Kurashima, T. Horiguchi, and M. Tateda, Appl. Opt. **29**, 2219 (1990).
12. Y. Mizuno, Z. He, and K. Hotate, Opt. Commun. **283**, 2438 (2010).
13. Y. Mizuno, Z. He, and K. Hotate, Appl. Phys. Express **2**, 112402 (2009).
14. T. Ishigure, Y. Koike, and J. W. Fleming, J. Lightwave Technol. **18**, 178 (2000).
15. R. M. Waxler, D. Horowitz, and A. Feldman, Appl. Opt. **18**, 101 (1979).
16. D. D. Raftopoulos, D. Karapanos, and P. S. Theocaris, J. Phys. D **9**, 869 (1976).
17. S. Kiesel, K. Peters, T. Hassan, and M. Kowalsky, Meas. Sci. Technol. **18**, 3144 (2007).
18. M. Silva-Lopez, A. Fender, W. N. MacPherson, J. S. Barton, J. D. C. Jones, D. Zhao, H. Dobb, D. J. Webb, L. Zhang, and I. Bennion, Opt. Lett. **30**, 3129 (2005).
19. J. Saneyoshi, Y. Kikuchi, and O. Nomoto, *Handbook of Ultrasonic Technology* (Nikkan Kogyo, 1978), Chap. 5.